

## Exciton dephasing via phonon interactions in InAs quantum dots: Dependence on quantum confinement

P. Borri,\* W. Langbein,† and U. Woggon

*Experimentelle Physik IIb, Universität Dortmund, Otto-Hahn Str. 4, D-44221 Dortmund, Germany*

V. Stavarache, D. Reuter, and A. D. Wieck

*Angewandte Festkörperphysik, Ruhr-Universität Bochum, Universitätsstr. 150, D-44780 Bochum, Germany*

(Received 15 July 2004; revised manuscript received 27 October 2004; published 29 March 2005)

We report systematic measurements of the dephasing of the excitonic ground-state transition in a series of InGaAs/GaAs quantum dots having different quantum confinement potentials. Using a highly sensitive four-wave mixing technique, we measure the polarization decay in the temperature range from 5 to 120 K on nine samples having the energy distance from the dot ground-state transition to the wetting layer continuum (confinement energy) tuned from 332 to 69 meV by thermal annealing. The width and the weight of the zero-phonon line in the homogeneous line shape are inferred from the measured polarization decay and are discussed within the framework of recent theoretical models of the exciton-acoustic phonon interaction in quantum dots. The weight of the zero-phonon line is found to decrease with increasing lattice temperature and confinement energy, consistently with theoretical predictions by the independent Boson model. The temperature-dependent width of the zero-phonon line is well reproduced by a thermally activated behavior having two constant activation energies of 6 and 28 meV, independent of confinement energy. Only the coefficient to the 6-meV activation energy shows a systematic increase with increasing confinement energy. These findings rule out that the process of one-phonon absorption from the excitonic ground state into higher energy states is the underlying dephasing mechanism.

DOI: 10.1103/PhysRevB.71.115328

PACS number(s): 78.67.Hc, 78.47.+p, 63.22.+m

### I. INTRODUCTION

The interband polarization optically driven by a coherent light field in a semiconductor quantum dot (QD) involves the coherent superposition of Coulomb-correlated valence- and conduction-band states (excitonic polarization). The study of the dephasing time  $T_2$  of the excitonic polarization in QDs has recently received a renewed attention for its implication in the applications of QDs for quantum information processing.<sup>1</sup> In this respect epitaxially grown InGaAs/GaAs QDs are particularly interesting, since they show very high crystalline and optical quality and long dephasing times of the excitonic ground-state transition in the nanosecond range at low temperature ( $\sim 5$  K).<sup>2</sup> These QDs have allowed for experimental achievements such as the coherent manipulation of the excitonic population via resonant Rabi rotations and the generation of nonclassical light.<sup>3</sup>

Among the physical mechanisms responsible for the dephasing, the interaction of excitons with phonons in QDs is a topic intensively discussed in the literature and still under debate. In particular, in strongly confined epitaxially grown InGaAs/GaAs QDs an unusual nonexponential decay of the optically driven polarization was recently observed,<sup>2</sup> corresponding to a non-Lorentzian homogeneous line shape with a narrow line superimposed to a broad band, that has stimulated a number of theoretical works.<sup>4–10</sup> A clear understanding of the physical processes governing this unusual dephasing is of fundamental interest and of key importance to predict and control the decoherence for applications of QDs in quantum computing.

Recent theoretical works<sup>4–10</sup> describe a non-Lorentzian homogeneous line shape for excitons in strongly confined

QDs following a similar discussion as for electrons localized on lattice defects in bulk semiconductors (see, e.g., Ref. 11). The starting point of this treatment considers that the crystal ground state and the state where the localized exciton is optically created correspond to different adiabatic potentials for the nuclear motion. The modification of the adiabatic potential for the nuclear motion due to the electronic excitation can be expressed in different orders of the nuclear displacement coordinates. A shift of the potential minimum in the lattice displacement coordinates is a linear contribution while a change of the curvature is a quadratic contribution. A relative shift between the potential minima in the absence and in the presence of the localized exciton implies that optical transitions can occur with absorption and emission of phonons, similar to the electronic transitions in molecules showing rotovibrational bands governed by the Franck-Condon principle.

The mathematical treatment of an exciton-phonon interaction which is linear in the phonon displacement operators and does not involve excited excitonic states is given in Refs. 4, 5, and 12. In this case the form of the exciton-phonon Hamiltonian is reduced to that of the independent Boson model and allows for an analytical solution giving polaronic eigenstates. The exciton-phonon interaction in this form does not lead to a change of the excitonic population and thus accounts only for pure dephasing. Note that the importance of pure dephasing via exciton-phonon interaction in semiconductor quantum dots was already pointed out in earlier works<sup>13,14</sup> which used perturbation theory as opposed to the analytical solution of the independent Boson model. When LO phonons are considered, the absorption (emission) spec-

tra calculated for (In,Ga)As QDs exhibit several side lines, separated by the LO phonon frequencies, above (below) a central line, consistently with experiments.<sup>15</sup> When acoustic phonons are taken into account as a continuum of bulklike modes, which is a good approximation for dots embedded in a matrix with similar elastic properties such as (In,Ga)As QDs on (Ga,Al)As barriers, the central line decomposes into a sharp zero-phonon line (ZPL) and a broad band caused by the continuum of acoustic-phonon assisted transitions, which at low temperature forms a shoulder toward high (low) energies in the absorption (emission) spectrum. The width of the broad band increases with decreasing size of the dot (i.e., of the excitonic wave function).<sup>12</sup> The weight of the ZPL can be used to introduce a Huang-Rhys factor for the exciton-acoustic phonon coupling, which increases with decreasing size of the dot or increasing temperature.<sup>5,12</sup>

This composite non-Lorentzian line shape is expected to be more visible in strongly confined dots and was experimentally observed in the photoluminescence spectra of II-VI epitaxially grown QDs,<sup>12</sup> while it is hardly resolved for excitons weakly confined by the lateral disorder in narrow GaAs quantum wells.<sup>17,18</sup> In InGaAs/GaAs self-assembled QDs the non-Lorentzian homogeneous line shape was experimentally indicated by a strongly nonexponential decay of the optically driven polarization measured in time domain, consisting of an initial fast decay over a few picoseconds (corresponding to the broad band in spectral domain) followed by a long exponential decay over several hundred picoseconds (corresponding to the ZPL).<sup>2</sup> Only very recently the non-Lorentzian line shape was directly observed in the photoluminescence spectra of single InAs QDs.<sup>19,20</sup> In fact, the detection of a spectral line shape consisting of a narrow ZPL (in the  $\mu\text{eV}$  range) on top of a broad band several meV wide and with an area of less than 20% of the total area of the line, as is the case for InGaAs QDs at low temperature,<sup>2</sup> requires a large signal-to-noise ratio not easily achieved in single-dot photoluminescence experiments. Note also that the spectral overlap of broad bands from adjacent exciton lines gives rise to a spectrally flat background sometimes reported in microphotoluminescence studies.<sup>21,22</sup>

The theoretical description recently proposed of the exciton-acoustic phonon interaction giving rise to a non-Lorentzian homogeneous line shape is able to explain the experimental observation of a decrease of the ZPL weight with increasing temperature.<sup>4,5,12,23</sup> However, within the independent Boson model the ZPL is *unbroadened*, in clear contrast to the experimentally observed broadening of the ZPL which increases with increasing temperature.<sup>2,24</sup> For a theoretical description of the width of the ZPL, two types of dephasing mechanisms can be distinguished: (i) population transfer such as radiative recombination and phonon-assisted transitions toward other confined electronic levels, and (ii) pure dephasing processes that do not change the carrier occupation. In recent literature, extensions of the independent Boson model with a quadratic coupling in the phonon displacement are reported in order to derive a temperature-dependent broadening of the ZPL due to pure dephasing.<sup>8,10,16</sup> However, a comparison with the experimental data for InGaAs QDs still gives no quantitative agreement.<sup>10</sup> On the other hand, an interpretation of the ZPL

width in terms of inelastic dephasing processes via radiative recombination and phonon-assisted absorption into higher electronic states<sup>2</sup> was not supported by a systematic experimental study, e.g., as a function of the electronic energy-level spacing in the QDs.

In this work, we have performed a systematic experimental study of the exciton dephasing and its temperature dependence in a series of InAs/GaAs QDs having different energy distances from the excitonic ground-state transition in the QD and the wetting layer continuum (confinement energy). Using a four-wave mixing (FWM) technique we measured the polarization decay of the ground-state excitonic transition in the temperature range from 5 to 120 K on nine samples having confinement energies ranging from 332 to 69 meV. The width and the weight of the ZPL at different lattice temperatures are inferred from the measured polarization decay. We find that the weight of the ZPL follows a dependence on temperature and confinement energy in agreement with the expectations of the independent Boson model. On the other hand, the width of the ZPL shows a thermally activated behavior with two activation energies of 6 and 28 meV *independent of confinement energy*. This finding contrasts an interpretation in terms of one-phonon absorption processes from the ground state toward higher electronic levels and should stimulate further theoretical work on pure dephasing processes beyond the independent Boson model.

## II. SAMPLES AND EXPERIMENT

The investigated samples are planar structures containing InAs/GaAs self-assembled QDs grown on a GaAs(100) substrate using molecular-beam epitaxy. Ten stacked layers of QDs were grown separated by 100-nm GaAs spacing layers and with  $2\text{--}3 \times 10^{10} \text{ cm}^{-2}$  areal density, i.e., quantum-mechanically uncoupled. QDs were obtained by deposition of a nominal coverage of 2.1 monolayers of InAs at a substrate temperature of 515 °C resulting in the formation of InAs islands that were overgrown with 8-nm GaAs at a reduced substrate temperature of 505 °C. After the growth, nine pieces of the wafer were subjected to rapid thermal annealing of 30 s at temperature ranging from 800 to 960 °C in order to decrease the depth of the in-plane confining potential due to the thermally induced In diffusion in the growth direction.<sup>26</sup> Figure 10 shows the optical density of states (DOS) of some of the samples obtained by dividing room-temperature photoluminescence spectra with the Maxwell-Boltzmann thermal distribution function,<sup>25</sup> a procedure which assumes thermal equilibrium and low excitation density. The first two peaks in the DOS correspond to the ground (GS) and first excited (ES) excitonic transitions, showing a sizeable inhomogeneous and also homogeneous broadening at room temperature.<sup>2</sup> The thermal annealing strongly shifts the GS excitonic transition to higher energies, while the wetting layer (WL) transition shifts only slightly. Therefore the energy distance from the GS to the WL transition is tuned in the QD series from 332 to 69 meV. This energy distance will be called in the following confinement energy  $E_c$ .

The FWM experiment is performed using Fourier-limited pulses of  $\sim 100$ -fs duration at 76-MHz repetition rate, in

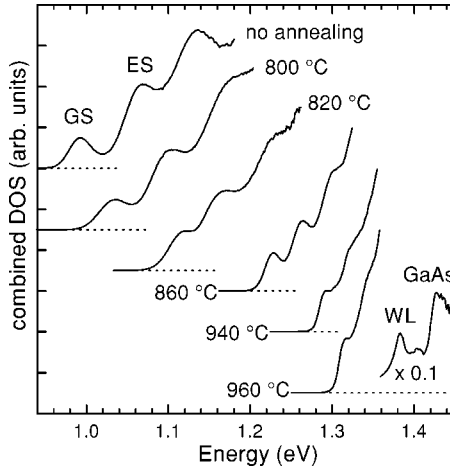


FIG. 1. Combined density of states inferred from room-temperature photoluminescence spectra in a series of InAs quantum dots subject to thermal annealing for 30 s at the indicated temperatures. Curves are vertically displaced for clarity. The first two peaks corresponding to the excitonic ground-state (GS) and first excited-state (ES) transitions are indicated. The wetting layer (WL) and GaAs transitions measured on the dots annealed at 960 °C are also shown.

resonance with the center of the inhomogeneously broadened GS transition. Two exciting pulses 1,2 with variable relative delay time  $\tau$  propagate along two different incident directions  $\vec{k}_{1,2}$ , with pulse 1 leading pulse 2 for  $\tau > 0$ . The FWM signal was detected along  $2\vec{k}_2 - \vec{k}_1$  in transmission geometry. The intensities of the exciting pulses were chosen to give rise to FWM in the third-order regime. In order to distinguish FWM intensities down to 15 orders of magnitude lower in intensity than the transmitted beams along  $\vec{k}_{1,2}$ , we additionally used a heterodyne detection technique similar to the one discussed in our previous work.<sup>2</sup> In this technique, the pulse 1 (2) is frequency shifted by a radiofrequency  $\omega_1$  ( $\omega_2$ ) and the interference of the FWM signal with an unshifted reference pulse is detected at  $2\omega_2 - \omega_1$  using high-frequency photodiodes and a lock-in amplifier.<sup>27</sup> In this way, the FWM field amplitude is measured via its interference with the field of the reference pulse. The exciting pulses were either co-circularly polarized in order to suppress biexcitonic contributions in the FWM dynamics at small delays, or co-linearly polarized to suppress beats arising from the excitonic fine structure at long delays.<sup>28</sup> The samples were antireflection coated to inhibit multiple reflections and increase light coupling and were held in a cryostat at temperatures between 5 and 120 K.

### III. RESULTS AND DISCUSSION

The FWM signal of an inhomogeneously broadened ensemble of resonances is a photon echo in real time.<sup>29</sup> The time evolution of the polarization amplitude of an individual resonance, i.e., the (microscopic) dephasing, is monitored by the time-integrated photon echo as a function of the delay time  $\tau$  between the exciting pulses. In Fig. 2 the time-integrated FWM (TI FWM) field amplitude versus  $\tau$  is

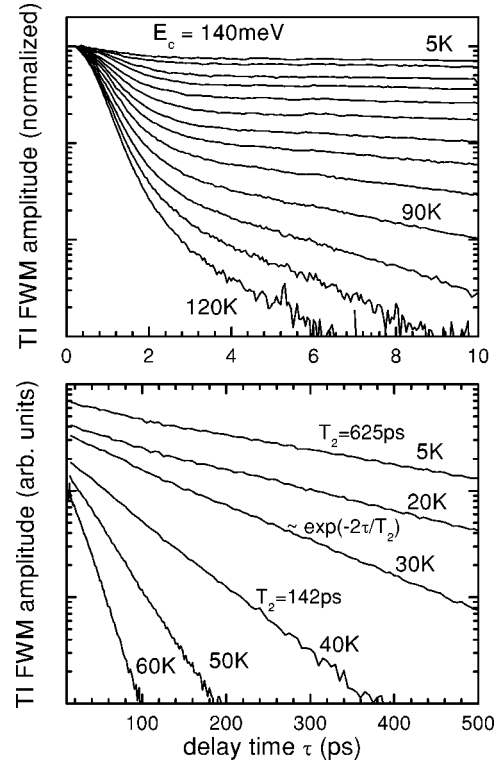


FIG. 2. Time-integrated four-wave mixing field amplitude vs delay time between the exciting pulses on InGaAs QDs with 140-meV confinement energy. Top: zoom over the initial 10-ps delay time for temperatures of 5, 10, 20, ..., 120 K in steps of 10 K. Circularly polarized excitation. Bottom: long delay dynamics at the indicated temperatures. Examples of the dephasing time  $T_2$  inferred from an exponential fit according to the indicated function are also shown for the data at 5 and 40 K. Linearly polarized excitation.

shown for a QD sample with a confinement energy of 140 meV in the temperature range from 5 to 120 K. With increasing temperature, the polarization decay becomes faster and strongly nonexponential. The nonexponential behavior is consistent with our previous findings on InGaAs/GaAs QDs,<sup>2</sup> and is explained by the independent Boson model as the manifestation in time domain of a non-Lorentzian homogeneous line shape with a narrow ZPL and a broad band from pure dephasing via exciton-acoustic phonon interactions.<sup>4,6,7</sup>

#### A. Weight of the zero-phonon line

The weight  $Z$  of the ZPL is defined as the area fraction of the ZPL in the linear absorption spectrum.<sup>5</sup> To extract it from FWM experiments, we use the results of Refs. 6 and 7, in which the time-resolved FWM field is calculated within the independent Boson model for infinitely short exciting pulses. Assuming, furthermore, an infinitely large inhomogeneous broadening (i.e., an infinitely short photon echo in real time), the TI FWM field envelope  $\bar{G}_\infty(\tau)$  in a photon echo experiment (normalized to 1 at  $\tau=0$ ) is derived. Both assumptions are valid approximations if the pulse and the photon echo durations are much shorter than the intrinsic acoustic phonon dynamics. These conditions are met in our experiment, in

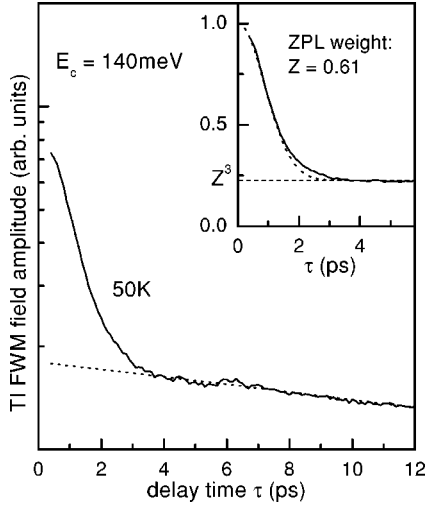


FIG. 3. Time-integrated field amplitude at 50 K together with an exponential fit of the dynamics at long delay times (dotted line). The initial FWM dynamics divided by the exponential fit, is shown in the inset together with a Gaussian function (dotted line) fitting to the initial decay. The asymptotic value at large delay (dashed line) is used to calculate the ZPL weight, as indicated.

which the inhomogeneous broadening and the Fourier-limited pulse spectra are much wider than the acoustic-phonon band. We therefore can use the results of Ref. 7 for  $\bar{G}_\infty(\tau)$  and for the envelope function of the linear polarization in real time  $G_{\text{lin}}(t)$ :

$$\bar{G}_\infty(\tau \rightarrow \infty) = |G_{\text{lin}}(t \rightarrow \infty)|^3 = Z^3. \quad (1)$$

To compare Eq. (1) with the experiment, we have to remove from the experimental data the effect of the long time decay of the polarization (i.e., the ZPL width) not included in Eq. (1). We can do so by dividing the data through the observed exponential decay of the ZPL (see dotted line in Fig. 3), which results in the solid curve shown in the inset. This procedure assumes that the polarization decay can be factorized in the product of the fast decay predicted by the independent Boson model with the long exponential decay,<sup>5</sup> i.e., that the same dephasing of the ZPL is present also in the phonon-assisted transitions of the independent Boson model. Moreover, since for  $|\tau| < 300$  fs the data are dominated by nonresonant FWM in the GaAs barrier, the TI FWM amplitude at  $\tau=0$ , which is needed to calculate the normalized function  $\bar{G}_\infty(\tau)$ , was estimated by fitting the initial decay with a Gaussian (dotted curve shown in the inset of Fig. 3). The deduced ZPL weight  $Z$  is indicated in the inset of Fig. 3.

Using this procedure, the temperature-dependent ZPL weight was determined for three QD samples having different confinement energies (see Fig. 4). Within the independent Boson model, it is expected that the ZPL weight decreases with increasing temperature and with decreasing extension of the excitonic wave function.<sup>4,5,12</sup> This is consistent with the measured ZPL weight, keeping in mind that a decreasing confinement energy results in an increase in the size of the excitonic wave function.<sup>26</sup> A comparison of both the amplitude and the time constant of the initial fast FWM decay

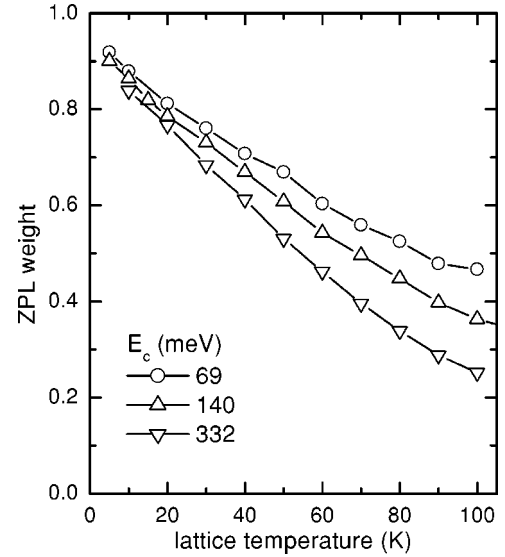


FIG. 4. ZPL weight vs lattice temperature for three QD samples with different confinement energies as indicated.

dynamics with the prediction of the independent Boson model is reported in Ref. 23 for two of the samples, and shows a quantitative agreement.

### B. Width of the zero-phonon line

After the initial decay over a few picoseconds, the polarization dynamics is characterized by a long exponential decay (see Fig. 2) with a dephasing time  $T_2$  inversely proportional to the width of the ZPL. In Fig. 5 the full width at half maximum  $\gamma = 2\hbar/T_2$  of the ZPL is shown versus temperature for four QD samples having different confinement energies as indicated. The increase of  $\gamma$  with increasing temperature

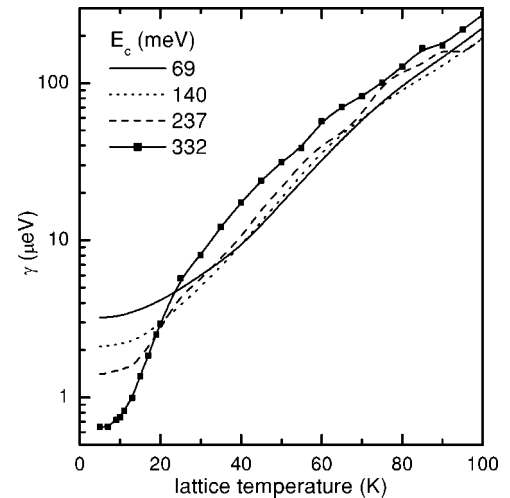


FIG. 5. Homogeneous broadening (full width at half maximum) of the ZPL deduced by the dephasing time  $T_2$  extracted from the exponential decay of the polarization at long times ( $\gamma = 2\hbar/T_2$ ), in four QD samples with different confinement energies as indicated. For clarity, data points (symbols) are shown only for one sample, while interpolating curves are given for the other samples.

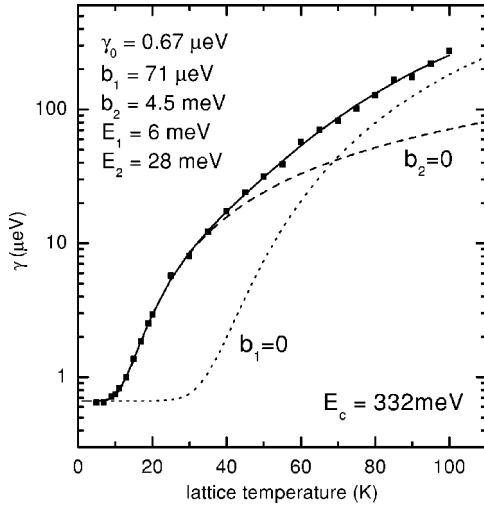


FIG. 6. Homogeneous broadening of the ZPL vs temperature (square points) in the QDs having 332-meV confinement energy, together with a fit to the data (solid line) according to Eq. (1). The parameters deduced from the fit are indicated. The contribution of the activated term with  $E_1$  ( $E_2$ ) in Eq. (2) is given as dashed (dotted) line.

exhibits a systematic dependence with  $E_c$ . In particular, the low-temperature value of  $\gamma$  is increasing with decreasing  $E_c$ . On the other hand, strongly confined QDs show a more pronounced thermally activated increase of  $\gamma$  giving rise to a crossing of the curves of Fig. 5.

The temperature dependence of the homogeneous linewidth of the ground-state exciton in semiconductor quantum wells ( $\gamma^{\text{QW}}$ ) was calculated by considering the probability of one-phonon absorption processes from the optically active excitonic ground state into higher energy states,<sup>30,31</sup> for which the dependence  $\gamma^{\text{QW}} = \gamma_0 + aT + b / [\exp(\hbar\omega_{\text{LO}}/k_B T) - 1]$  was predicted. The linear term  $aT$  is due to the absorption of acoustic phonons of energies much smaller than  $k_B T$ , while the last term is due to the absorption of longitudinal optical (LO) phonons and is proportional to the Bose function for the LO-phonon occupation number, with the LO-phonon energy  $\hbar\omega_{\text{LO}}$ . In semiconductor quantum dots, one-phonon absorption from the excitonic ground state occurs toward energetically well separated excited states. The individual transitions consequently should contribute to the temperature dependence of  $\gamma$  with Bose functions having activation energies equal to the energy separation between the ground and the involved excited states.<sup>32</sup>

We found that a good fit to the temperature dependence of  $\gamma$  for *all* investigated QDs is indeed obtained using two Bose functions with activation energies  $E_1$  and  $E_2$  and coefficients  $b_1$  and  $b_2$ :

$$\gamma = \gamma_0 + b_1 \frac{1}{e^{E_1/k_B T} - 1} + b_2 \frac{1}{e^{E_2/k_B T} - 1}, \quad (2)$$

where  $\gamma_0$  represents a temperature-independent broadening. An example of this fit is shown in Fig. 6 for the QDs having 332-meV confinement energy. The parameters used in the fit are indicated in the figure. Remarkably, the activation ener-

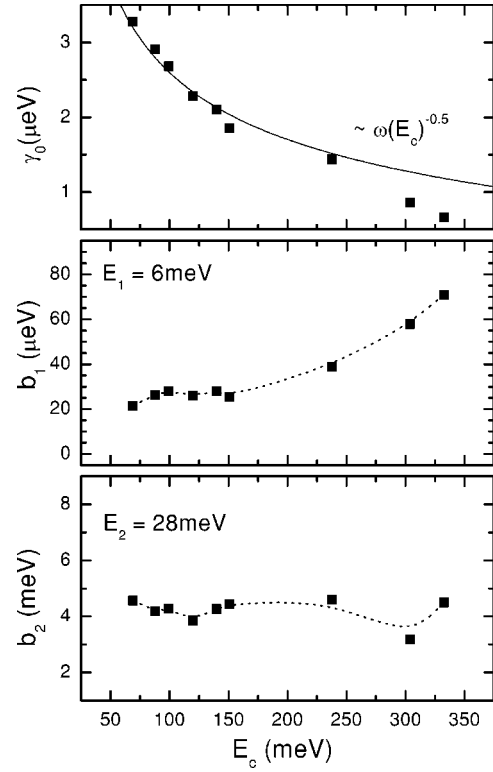


FIG. 7. Top: zero-temperature extrapolated homogeneous broadening of the ZPL (square symbols) vs confinement energy compared with a curve (solid line) proportional to the inverse square root of the confinement energy  $E_c$  times the optical transition frequency  $\omega$ . Middle (bottom): coefficient  $b_1$  ( $b_2$ ) of the thermally activated increase of the ZPL width with activation energy  $E_1$  ( $E_2$ ) vs confinement energy. Dotted lines are guides to the eye. The size of the symbols is equal to or bigger than the error bars of the parameters from the fits.

gies  $E_1$  and  $E_2$  were found to be constant within error (10%) for all investigated samples, i.e., independent of the confinement energy. We have therefore fixed  $E_1 = 6$  meV and  $E_2 = 28$  meV for all fits. The dependence of the remaining three parameters on  $E_c$  is summarized in Fig. 7, revealing a systematic decrease of  $\gamma_0$  and increase of  $b_1$  with increasing  $E_c$ . When fitting the data with Eq. (2) including a linear term  $aT$ , we find in all samples that  $a = 0 \pm 0.02$   $\mu\text{eV}/\text{K}$ , i.e., the linear term is zero within error.

The zero-temperature dephasing rate  $\gamma_0$  is given by the radiative lifetime  $T_{\text{rad}}$  (i.e.,  $\gamma_0 = \hbar/T_{\text{rad}}$ ), as we have experimentally demonstrated<sup>33</sup> by comparing the polarization decay with the strength of the FWM signal and thus of the transition dipole moment. The radiative lifetime in InGaAs QDs depends on the electron-hole wave-function overlap and on the exciton coherence volume.<sup>34</sup> Both quantities are influenced by the annealing. In particular, the reduction of the in-plane confinement potential by annealing<sup>26</sup> results in an increased extension of the excitonic wave function in plane and thus in an increased exciton coherence area. If the in-plane exciton confinement potential is approximated by a two-dimensional harmonic oscillator potential of depth  $E_c$  (neglecting the zero-point quantization energy) reaching the wetting layer at a fixed diameter, the coherence area can be

shown<sup>33</sup> to scale like  $1/\sqrt{E_c}$ . Consequently the radiative decay scales like [see Eqs. (45) and (46) in Ref. 35 or Eq. (5.62) in Ref. 34]  $\omega\sqrt{E_c}$  where  $\omega$  is the frequency of the optical transition, i.e.,  $\hbar\omega = E_{\text{WL}} - E_c$  with  $E_{\text{WL}}$  the energy of the wetting layer transition. The solid line in the top part of Fig. 7 shows this trend which well reproduces the experimental dependence for confinement energies  $E_c < 200$  meV. The deviation at large confinement energies could be due to an asymmetry of the In distribution in the growth direction, resulting in a decreased electron-hole wave function overlap and thus in a decreased radiative rate. This asymmetry is removed in the first stage of annealing. Measurements of the biexciton binding energy in the same sample series are indeed consistent with the presence of an asymmetric In distribution in the growth direction which is symmetrized by annealing. An increase in the electron-hole wave function overlap in the initial stage of annealing also reduces the charge separation and thus results in a reduced repulsive exciton-exciton interaction and in an increased biexciton binding energy which we have measured.<sup>28</sup>

Concerning the temperature-dependent dephasing, we note that the activation energy  $E_2 = 28$  meV is close to the range of optical phonon energies (29–36 meV) observed in InGaAs QDs.<sup>36,37</sup> Optical phonons feature a density of states peaked at a certain energy. If the involved optical-phonon interaction would be a one-phonon absorption process, electronic excited states at the distance of the optical-phonon energy would have to be present. While for confinement energies less than 100 meV, this could be due to the continuum of hole states in the wetting layer, at larger confinement energies no such continuum is expected, in contrast to the observation of a rather constant coefficient  $b_2$  vs  $E_c$ . An alternative pure dephasing mechanism via elastic interaction with longitudinal optical phonons, which have a finite lifetime due to the decay into acoustic phonons, was discussed in Refs. 8 and 16. For a phonon lifetime smaller than the exciton dephasing time, which is the case in most of our measurements, a Lorentzian broadening is predicted, having a temperature dependence proportional to  $\bar{n}(\bar{n} + 1)$  with the phonon occupation  $\bar{n}$ . Since  $\bar{n} \ll 1$  in the measured temperature range, this dependence is similar to the one used in Eq. (2). Also the observed value of  $b_2$  is within an order of magnitude equal to the result of Ref. 16 for a similar QD structure, supporting the interpretation of the observed dephasing along these lines.

Turning to the activation energy  $E_1 = 6$  meV, we first note that acoustic phonons do not have a concentrated density of states at this energy. The phonon energy for transitions involving one-acoustic phonon absorption into higher energy states should thus be given by the discrete energy-level spacing in the QDs. In the investigated series of QDs, the energy separation from GS to ES transitions was measured to change from  $\sim 70$  to  $\sim 25$  meV with decreasing  $E_c$  from 332 to 69 meV. Our finding of a constant activation energy  $E_1$  therefore clearly contradicts the importance of such phonon absorption processes for the dephasing. Furthermore, acoustic phonons have a long lifetime, so that a discussion similar to the one mentioned above for the optical phonons is not likely. Recent theoretical models have suggested a broadening of the ZPL via pure dephasing mechanisms. In Ref. 5 a

temperature-dependent acoustic-phonon damping by lattice anharmonicities was introduced semiphenomenologically, resulting in an  $T^4$  low-temperature scaling of the dephasing, in qualitative agreement with the experimental data of Ref. 2. In Ref. 38 an acoustic-phonon damping by surface roughness scattering is introduced, leading to a zero-temperature offset and a linear temperature dependence of the exciton dephasing, in contrast to our present experimental observations. In Ref. 10 it is shown that phonon-assisted virtual transitions into higher electronic states can be cast into an effective quadratic coupling in the phonon displacement, which is known to lead to a temperature-dependent pure dephasing of the ZPL for a thermal phonon population. This approach predicts a dephasing reproducing the main features of the temperature dependence observed here, but a quantitative comparison of the confinement energy dependence is not available. In view of this unsettled discussion about the relevant dephasing mechanisms, we expect that the experimental results presented here will help the verification of the various theoretical models. It remains the experimental finding that the coefficient  $b_1$  is increasing with increasing  $E_c$ . This behavior contradicts the intuitive idea that strongly confined QDs should have a homogeneous broadening less sensitive to temperature due to inhibited phonon-assisted transitions between confined electronic states and supports the importance of pure dephasing mechanisms.

When comparing the present results on the thermally activated broadening of the ZPL with published data on InGaAs QDs, one notes that previously a relevant linear increase ( $aT$ ) was found at low temperatures.<sup>2,22,24,39,40</sup> In this respect one has to consider the effect of dynamical broadening due to a spectral jitter of the QD transition. Experiments such as single-dot emission spectroscopy<sup>22,24,39,40</sup> are sensitive to the dynamical broadening during the integration time of seconds or more, while transient FWM photon echo spectroscopy<sup>2,39</sup> is sensitive to the dynamical broadening during the subnanosecond time span between excitation and echo formation only. Accordingly is the effect of the dynamical broadening on the single dot emission experiments by far larger than for the photon echo experiments. If the measured width of the ZPL is dominated by dynamical broadening, the measured temperature dependence can also reflect the influence of lattice temperature on the mechanisms responsible of the spectral jitter, which are not related to the homogeneous broadening from exciton-phonon interactions. For example, a change of the fluctuating charge densities near the QDs from carrier thermal escape would give rise to a temperature dependent fluctuating Stark shift and hence spectral jitter of the QD resonance. The largest coefficients  $a > 1$   $\mu\text{eV}/\text{K}$  are indeed reported for experiments significantly affected by dynamical broadening.<sup>40</sup> In Ref. 24, where the influence of the dynamical broadening on single-dot spectra was strongly reduced,  $a \approx 0.5$   $\mu\text{eV}/\text{K}$  was found. In our previous work using transient FWM,<sup>2</sup> we measured  $a = 0.22$   $\mu\text{eV}/\text{K}$  and the zero-temperature extrapolated ZPL broadening of 0.7  $\mu\text{eV}$  was consistent with the lifetime limit, so that we could exclude a significant influence of dynamical broadening. In Ref. 2 we attributed  $a$  to phonon-assisted transitions among the exciton fine-structure states. However, this interpretation appears to contradict recent measurements showing an exci-

ton spin-flip time much longer than the radiative lifetime.<sup>41</sup> A recent work relates the linear temperature dependence to structural details of surfaces in the QD surroundings resulting in a damping of the acoustic phonons through boundary scattering.<sup>38</sup> In general, a consistent physical understanding of the measured linear temperature dependence of the ZPL width in InGaAs QDs at low temperatures is not available at present. Considering the large scatter of the reported coefficients, it is likely to be due to extrinsic effects by the QD surroundings, rather than to the intrinsic electron-phonon interaction.

#### IV. SUMMARY

In summary, we have performed four-wave mixing measurements of the polarization decay in resonance with the excitonic ground-state transition in a series of annealed InAs/GaAs QDs having confinement energies ranging from 332 to 69 meV. The strongly nonexponential decay of the optically driven polarization is studied as a function of lattice temperature (from 5 to 120 K) and confinement energy. The corresponding non-Lorentzian homogeneous line shape shows a sharp zero-phonon line and a broad band, with a ratio between the ZPL area and the total area of the line (ZPL weight) that decreases with increasing temperature and confinement energy. This behavior is consistent with a descrip-

tion of the exciton acoustic-phonon interaction recently proposed in the literature within the independent Boson model. The temperature dependence of the width of the ZPL can be well described by a thermally activated behavior with two activation energies which are independent of the confinement energy. This latter result contradicts that the process of one-phonon absorption from the excitonic ground state into higher energy states is the underlying dephasing mechanism, and points towards the relevance of pure dephasing processes beyond the independent Boson model. These results should stimulate further theoretical work in the fundamental understanding of the exciton-phonon dephasing mechanisms in semiconductor quantum dots. Additionally, we found that while the more strongly confined QDs have a smaller exciton coherence volume and thus a reduced radiative broadening, they show a stronger temperature-activated homogeneous broadening as compared to less confined QDs. These findings reveal a tradeoff between strong and weak confinement in the achievement of a reduced decoherence and are important for the design QDs for applications in quantum information processing.

#### ACKNOWLEDGMENTS

This work was supported by DFG in the frame of Contract No. Wo477/17-1 and by the Ph.D. Program GK726.

\*Present address: Cardiff University, Biomedical Sciences Building, Museum Avenue, Cardiff CF10 3US, Wales, UK; email address: BorriP@Cardiff.ac.uk

<sup>†</sup>Present address: Department of Physics and Astronomy, Cardiff University, 5 The Parade, Cardiff CF24 3YB, UK; email address: LangbeinWW@Cardiff.ac.uk

<sup>1</sup>Pochung Chen, C. Piermarocchi, and L. J. Sham, Phys. Rev. Lett. **87**, 067401 (2001).

<sup>2</sup>P. Borri, W. Langbein, S. Schneider, U. Woggon, R. L. Sellin, D. Ouyang, and D. Bimberg, Phys. Rev. Lett. **87**, 157401 (2001).

<sup>3</sup>*Single Quantum Dots—Fundamentals, Applications and New Concepts*, Topics in Applied Physics Vol. 90, edited by Peter Michler (Springer-Verlag, Berlin, 2003).

<sup>4</sup>B. Krummheuer, V. M. Axt, and T. Kuhn, Phys. Rev. B **65**, 195313 (2002).

<sup>5</sup>R. Zimmermann and E. Runge, in *Proceedings of the 26th International Conference on the Physics of Semiconductors*, edited by J. H. Davies and A. R. Long (Institute of Physics Publishing, Bristol, UK, 2002), p. M3.1.

<sup>6</sup>A. Vagov, V. M. Axt, and T. Kuhn, Phys. Rev. B **66**, 165312 (2002).

<sup>7</sup>A. Vagov, V. M. Axt, and T. Kuhn, Phys. Rev. B **67**, 115338 (2003).

<sup>8</sup>S. V. Goupalov, R. A. Suris, P. Lavallard, and D. S. Citrin, IEEE J. Sel. Top. Quantum Electron. **8**, 1009 (2002).

<sup>9</sup>J. Förstner, C. Weber, J. Danckwerts, and A. Knorr, Phys. Rev. Lett. **91**, 127401 (2003).

<sup>10</sup>E. A. Muljarov and R. Zimmermann, Phys. Rev. Lett. **93**, 237401 (2004).

<sup>11</sup>G. Mahan, *Many-Particle Physics* (Plenum, New York, 1990).

<sup>12</sup>L. Besombes, K. Kheng, L. Marsal, and H. Mariette, Phys. Rev. B **63**, 155307 (2001).

<sup>13</sup>T. Takagahara, Phys. Rev. B **60**, 2638 (1999).

<sup>14</sup>Xudong Fan, T. Takagahara, J. E. Cunningham, and Hailing Wang, Solid State Commun. **108**, 857 (1998).

<sup>15</sup>R. Heitz, I. Mukhametzhanov, O. Stier, A. Madhukar, and D. Bimberg, Phys. Rev. Lett. **83**, 4654 (1999).

<sup>16</sup>A. V. Uskov, A.-P. Jauho, B. Tromborg, J. Mørk, and R. Lang, Phys. Rev. Lett. **85**, 1516 (2000).

<sup>17</sup>J. Guest, T. H. Stievater, Gang Chen, E. A. Tabak, B. G. Orr, D. G. Steel, D. Gammon, and D. S. Katzer, Science **293**, 2224 (2001).

<sup>18</sup>E. Peter, J. Hours, P. Senellart, A. Vasanelli, A. Cavanna, J. Bloch, and J. M. Gérard, Phys. Rev. B **69**, 041307(R) (2004).

<sup>19</sup>I. Favero, G. Cassabois, R. Ferreira, D. Darson, C. Voisin, J. Tignon, C. Delalande, G. Bastard, Ph. Roussignol, and J. M. Gérard, Phys. Rev. B **68**, 233301 (2003).

<sup>20</sup>B. Urbaszek, E. J. McGhee, M. Krüger, R. J. Warburton, K. Karrai, T. Amand, B. D. Gerardot, P. M. Petroff, and J. M. Garcia, Phys. Rev. B **69**, 035304 (2004).

<sup>21</sup>K. Ota, N. Usami, and Y. Shiraki, Physica E (Amsterdam) **2**, 573 (1998).

<sup>22</sup>K. Leosson, J. R. Jensen, J. M. Hvam, and W. Langbein, Phys. Status Solidi B **221**, 49 (2000).

<sup>23</sup>A. Vagov, V. M. Axt, T. Kuhn, W. Langbein, P. Borri, and U. Woggon, Phys. Rev. B **70**, 201305(R) (2004).

<sup>24</sup>M. Bayer and A. Forchel, Phys. Rev. B **65**, 041308 (2002).

<sup>25</sup>Massimo Gurioli, Anna Vinatieri, Juan Martinez-Pastor, and Mar-

- cello Colocci, Phys. Rev. B **50**, 11 817 (1994).
- <sup>26</sup>S. Fafard and C. Ni. Allen, Appl. Phys. Lett. **75**, 2374 (1999).
- <sup>27</sup>Paola Borri, in *Nano-Optoelectronics: Concepts, Physics and Devices, Nanoscience and Technology*, edited by M. Grundmann (Springer-Verlag, Berlin, 2002), pp. 411–430.
- <sup>28</sup>W. Langbein, P. Borri, U. Woggon, V. Stavarache, D. Reuter, and A. D. Wieck, Phys. Rev. B **69**, 161301(R) (2004).
- <sup>29</sup>J. Shah, in *Ultrafast Spectroscopy of Semiconductors and Semiconductor Nanostructures* (Springer, Berlin, 1996).
- <sup>30</sup>S. Rudin and T. L. Reinecke, Phys. Rev. B **41**, 3017 (1990).
- <sup>31</sup>P. Borri, W. Langbein, J. M. Hvam, and F. Martelli, Phys. Rev. B **59**, 2215 (1999).
- <sup>32</sup>D. Gammon, E. S. Snow, B. V. Shanabrook, D. S. Katzer, and D. Park, Science **273**, 87 (1996).
- <sup>33</sup>W. Langbein, P. Borri, U. Woggon, V. Stavarache, D. Reuter, and A. D. Wieck, Phys. Rev. B **70**, 033301 (2004).
- <sup>34</sup>D. Bimberg, M. Grundmann, and N. N. Ledentsov, *Quantum Dot Heterostructures* (John Wiley and Sons, Chichester, 1999).
- <sup>35</sup>M. Sugawara, Phys. Rev. B **51**, 10 743 (1995).
- <sup>36</sup>R. Heitz, M. Veit, N. N. Ledentsov, A. Hoffmann, D. Bimberg, V. M. Ustinov, P. S. Kop'ev, and Zh. I. Alferov, Phys. Rev. B **56**, 10 435 (1997).
- <sup>37</sup>R. Heitz, H. Born, A. Hoffmann, D. Bimberg, I. Mukhametzhanov, and A. Madhukar, Appl. Phys. Lett. **77**, 3746 (2000).
- <sup>38</sup>G. Ortner, D. R. Yakovlev, M. Bayer, S. Rudin, T. L. Reinecke, S. Fafard, Z. Wasilewski, and P. Hawrylak, Phys. Rev. B **70**, 201301(R) (2004).
- <sup>39</sup>D. Birkedal, K. Leosson, and J. M. Hvam, Phys. Rev. Lett. **87**, 227401 (2001).
- <sup>40</sup>C. Kammerer, C. Voisin, G. Cassabois, C. Delalande, Ph. Rousignol, F. Klopff, J. P. Reithmaier, A. Forchel, and J. M. Gérard, Phys. Rev. B **66**, 041306 (2002).
- <sup>41</sup>M. Paillard, X. Marie, R. Renucci, T. Amand, A. Jbeli, and J. M. Gérard, Phys. Rev. Lett. **86**, 1634 (2001).